Dual Mode Controller-Based Solar Photovoltaic Simulator for True PV Characteristics
Simulateur photovoltaïque solaire basé sur un contrôler double modes pour des vraies caractéristiques d'un PV

Umesh K. Shinde, *Member, IEEE*, Sumant G. Kadwane, *Senior Member, IEEE*, Ritesh Kumar Keshri, *Senior Member, IEEE*, S. P. Gawande, *Member, IEEE*

***Abstract*— Integration of solar photovoltaic (PV) panels with existing utilities requires effectively controlled converters. While developing and testing such converters, it is difficult to test them with actually installed PV panels owing to unavailability of practical onsite conditions for all the time. For such cases, PV simulators are preferred, which are required to exhibit PV system behavior under working conditions without the use of real outdoor installation. This reduces the time and cost of experimentation. In this paper, a real-time PV simulator based on a dc–dc buck converter is investigated to obtain true PV characteristics. The practical difficulty with PV simulators is that they often get oscillations in the constant current region or constant voltage region of PV characteristics, particularly when the controller is designed using a low-cost digital controller. This paper introduces a novel hysteresis controller to ensure effective operation in both these regions. This dual control strategy ensures effective control in both regions and provides smooth trajectories as per mathematical model or lookup table to mimic any PV characteristics under various temperatures and insolations with the use of the low-cost digital controller. The hardware prototype is constructed with the digital signal controller to demonstrate the efficacy of the proposed simulator.**

***Résumé*— L'intégration de panneaux solaires photovoltaïques (PV) avec des installations électriques existantes nécessite des convertisseurs contrôlés de façon efficace. Tout en développant et en testant de tels convertisseurs, il est difficile de les tester avec des panneaux photovoltaïques réellement installés en raison de l'indisponibilité de conditions pratiques sur place pour tout le temps. Dans de tels cas, les simulateurs photovoltaïques sont préférés, qui sont nécessaires pour présenter le comportement du système photovoltaïque dans des conditions de travail sans utilisation d'une installation extérieure réelle. Cela réduit le temps et le coût de l'expérimentation. Dans cet article, un simulateur PV en temps réel basé sur un convertisseur hacheur série cc-cc est étudié pour obtenir des vraies caractéristiques d'un PV. La difficulté pratique avec les simulateurs photovoltaïques est qu'ils produisent souvent des oscillations dans la région du courant constant ou la région de la tension constante des caractéristiques PV, en particulier lorsque le contrôleur est conçu à l'aide d'un contrôleur numérique à faible coût. Cet article présente un nouveau contrôleur d'hystérésis pour assurer un fonctionnement efficace dans ces deux régions. Cette double stratégies de contrôle assure un contrôle efficace dans les deux régions et fournit des trajectoires lisses selon un modèle mathématique ou une table de consultation pour imiter toutes les caractéristiques de PV sous différentes températures et des insolations avec l'utilisation du contrôleur numérique à faible coût. Le prototype du matériel est construit avec le contrôleur de signal numérique pour démontrer l'efficacité du simulateur proposé.**

***Index Terms*— DC–DC converter, digital signal controller, photovoltaic (PV), pulsewidth modulation, simulator.**

I. Introduction

With increasing concerns about fossil fuel deficit, ever increasing oil prices, global warming, and damage to the environment and ecosystem, the promising alternative is to develop renewable energy-based systems with high efficiency and low emission. Among the renewable energy resources, the energy through the photovoltaic (PV) effect can be considered as one of the most essential and sustainable resources, because of the abundance and attainability of solar radiant energy [1]. Regardless of the intermittency of sunlight, solar energy is widely available and completely free of cost. Recently, the PV array system is recognized and widely uti-

Manuscript received January 31, 2017; accepted May 21, 2017. Date of current version September 28, 2017. *(Corresponding author: Umesh K. Shinde.)*

U. K. Shinde is with the Department of Electrical Engineering, Bhivarabai Sawant College of Engineering and Research, Pune, India (e-mail: ukshinde@yahoo.com).

S. G. Kadwane and S. P. Gawande are with the Department of Electrical Engineering, Yeshwantrao Chavan College of Engineering, Nagpur, India (e-mail: sgkadwane@gmail.com; spgawande_18@yahoo.com).

R. K. Keshri is with the Department of Electrical Engineering, Visvesvaraya National Institute of Technology, Nagpur, India (e-mail: riteshkeshri@gmail.com).

Associate Editor managing this paper's review: Hilmi Turanli.

Color versions of one or more of the figures in this paper are available online at http://ieeexplore.ieee.org.

Digital Object Identifier 10.1109/CJECE.2017.2708721

0840-8688 © 2017 IEEE. Personal use is permitted, but republication/redistribution requires IEEE permission.
See http://www.ieee.org/publications_standards/publications/rights/index.html for more information.

Authorized licensed use limited to: Instituto Tecnologico de Costa Rica (ITCR). Downloaded on June 23,2021 at 22:29:15 UTC from IEEE Xplore. Restrictions apply.

lized in electric power applications. Even though the PV system is posed to its high capital fabrication cost and low conversion efficiency, this energy is a naturally viable energy supply with potentially long-term benefits [2]. Therefore, the research and development in extracting maximum power from the solar system and design an effective control strategy for such systems are essential from the power electronics point of view.

Mathematical models and MATLAB-based simulations of a PV cell have been presented in [3] and [4]. A low-cost implementation of the maximum power point tracking (MPPT) method has been investigated in the literature [5]. Various MPPT techniques have been investigated recently using perturb and observe, incremental conductance, and many other methods, for more than a decade but still, this topic is attracting interest for many researchers for the reliable and low-cost operation of the solar system [6]–[8]. MPPT methods require the tracking of maximum power point in the power versus voltage characteristics of the solar cell. When the entire panel is not exposed to direct sunlight, the characteristics have multiple peaks, and maximum power point cannot be tracked easily. Some topologies and algorithms to overcome this difficulty are proposed as in [9], but still, it is a matter of investigation for many researchers. The primary problem associated with the research of such systems is the need of huge space typically for 1 kWp with the size of the 5–8-m^2 panel. Also, other factors, such as dependence on atmospheric conditions, little flexibility, difficulties to emulate grid perturbations, and irradiation changes, make the development time larger.

In order to minimize the design duration of the controller, the PV simulator is required to facilitate real-time testing. The requirement of this paper is in terms of stable power supply that will mimic the characteristics of the solar cell, which is called a PV Simulator. This PV simulator should behave electrically similar to PV arrays, it should have little weight and less volume per watt, and it should be able to produce characteristics as per dependence on weather conditions. The PV simulator uses lookup-tables-based data or a generalized model of a PV cell to obtain the I–V characteristics, which are elaborated in [10]–[25].

Modeling and design of a resonant converter-based PV simulator for high-efficiency operation are presented in [15] and [16]. The current mode buck converter-based emulator has been proposed in [19] and [20]. In [21], the PV simulator is constructed by approximating the characteristics by straight lines and accordingly the equations of the lines are implemented in a microcontroller. The disadvantage of this method is that the simulator can be constructed for one characteristic of temperature and the effect of a change in insolation is difficult to address in such implementation. Analytical model-based emulators with the help of more sophisticated but costly digital controllers have been presented in [22] and [23]. Reconfigurable emulator for testing of partial shading effect has been presented in [24]. Also, dual mode controller has been presented in [25] operating in both current source and voltage source regions. However, it requires additional power electronic hardware to achieve this.

Therefore, in order to alleviate these limitations, this paper proposes hysteresis-based selection to implement a dual mode controller using a low-cost dsPIC processor without use of additional power hardware. Also, a systematic approach to modeling and hardware design of the solar simulator has been investigated. The accurate PV characteristics in both regions prove the efficacy of the proposed simulator.

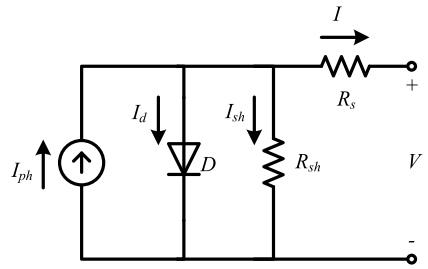

Fig. 1. Equivalent circuit of PV cell.

This paper is organized as follows. Section II presents the preamble of PV simulator design. The control scheme of dual mode controller is explained in Section III. Section IV covers the hardware specifications and scheme, while Section V covers the hardware results followed by a summary of conclusion in Section VI.

II. Photovoltaic Simulator Design

A. Mathematical Modeling of PV Cell

The most commonly used single diode equivalent of PV cell for generating the solar characteristics is shown in Fig. 1, which have been reported in the literature earlier [3], [4]. The terminal voltage and current of PV cell are related as

$$I = I_{\text{ph}} - I_s \left[\exp\left(\frac{q(V + IR_s)}{AkT} \right) - 1 \right] - \frac{(V + IR_s)}{R_{\text{sh}}} \tag{1}$$

where the symbols have their usual meanings.

The value of PV current I_{ph} depends on solar radiation and cell temperature as follows:

$$I_{\text{ph}} = [I_{\text{scr}} + k_i(T_c - T_r)] \frac{S}{1000} \tag{2}$$

where I_{scr} is the cell short circuit current at a reference temperature and radiation in Ampere; k_i is the short circuit current temperature coefficient; T_c is the cell temperature in Kelvin; T_r is the cell reference temperature in Kelvin, and S is the solar insolation in W/m^2.

The reverse saturation current I_S can be calculated from the cell reverse saturation current I_{rr} at a reference temperature and band gap voltage V_g as follows:

$$I_s = I_{\text{rr}} \left(\frac{T}{T_r} \right)^{3/A} \exp\left(\frac{V_g q}{Ak} \left(\frac{1}{T_r} - \frac{1}{T_c} \right) \right). \tag{3}$$

The value of I_{rr} in terms of short circuit current I_{scr} and open circuit voltage V_{ocr} at the same reference temperature is

$$I_{\text{rr}} = \frac{I_{\text{scr}}}{\exp\left(\frac{qV_{\text{ocr}}}{AkT_r} - 1 \right)}. \tag{4}$$

Using (1)–(4), the PV array is modeled for simulation and for hardware implementation as well.

Authorized licensed use limited to: Instituto Tecnologico de Costa Rica (ITCR). Downloaded on June 23,2021 at 22:29:15 UTC from IEEE Xplore. Restrictions apply.

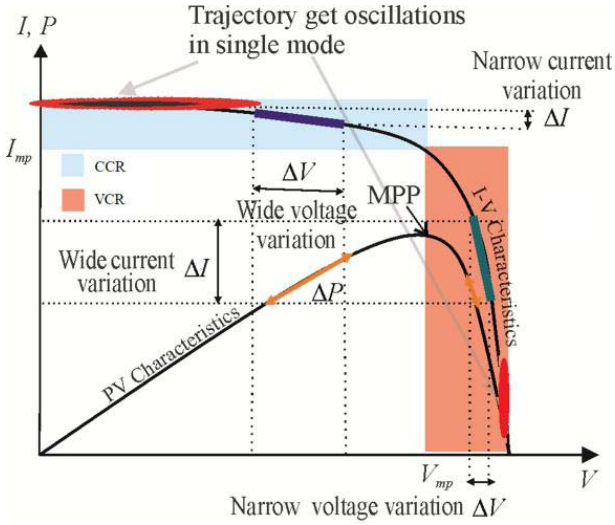

Fig. 2. Voltage and current variations in CCR and CVR.

B. Investigating the Necessity of Dual Mode Controller

Fig. 2 shows the I–V and P–V characteristics of solar cell for particular insolation and temperature. The characteristics are divided into two regions, namely the constant current region (CCR) and the constant voltage region (CVR). As shown in Fig. 2, CCR is characterized by large changes in terminal voltage of PV panel for small changes in current. Similarly, CVR is characterized by large changes in terminal current for small changes in terminal voltage. In practice, the current variations ΔI and voltage variations ΔV may be very small with the flat slope, and it may appear that $\Delta I \approx 0$ or $\Delta V \approx 0$ particularly while carrying computations with the fixed point digital processors. The region where trajectory may get stuck owing to inability to detect variations in current or voltages on PV trajectory is shown in Fig. 2. Therefore, it is required to effectively design the controller to operate in both modes to avoid getting struck in these regions and reproduce accurate PV characteristics. Furthermore, from Fig. 2, it is to be noted that CCR and CVR regions have the boundary point at $V = V_{\mathrm{mp}}$. In CCR, the converter should operate in current control mode (CCM) and in CVR, the converter should operate in voltage control mode (VCM).

C. Process of Simulator Hardware Interface

Basically, the simulator is a dc–dc converter, which emulates the characteristics of the solar panel. The input–output voltage or current ratio of the converter depends on duty ratio of PWM-fed to this converter. Owing to which if the controller is designed such that its duty ratio varies in accordance with the PV characteristics, then it will act as a PV Simulator. In this paper, the dc to dc step-down converter, which is one of the fundamental switching converters, is used for the prototype model.

Fig. 3 shows the process of simulator working and hardware interface. The digital signal controller dsPIC33FJ32M202 provides control signals in the form of PWM to dc–dc Buck Converter. The measurements of current and voltage are fed to ADC of the processor by proper analog conditioning. The

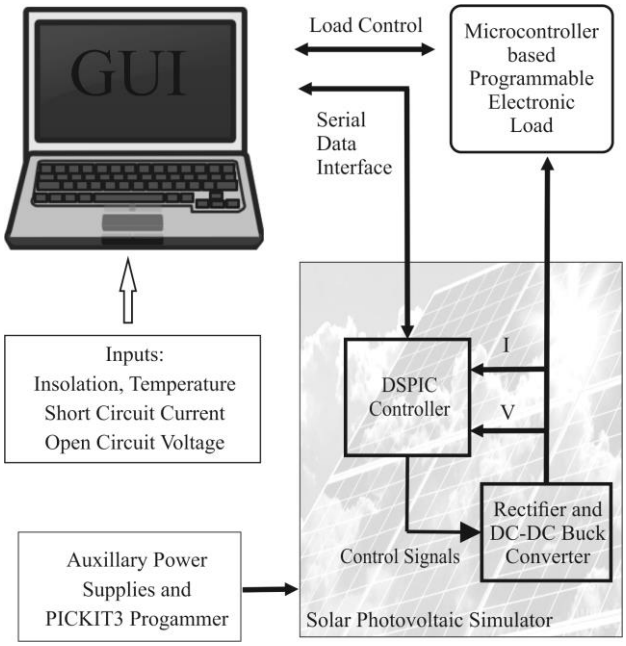

Fig. 3. Testing process and interfacing simulator.

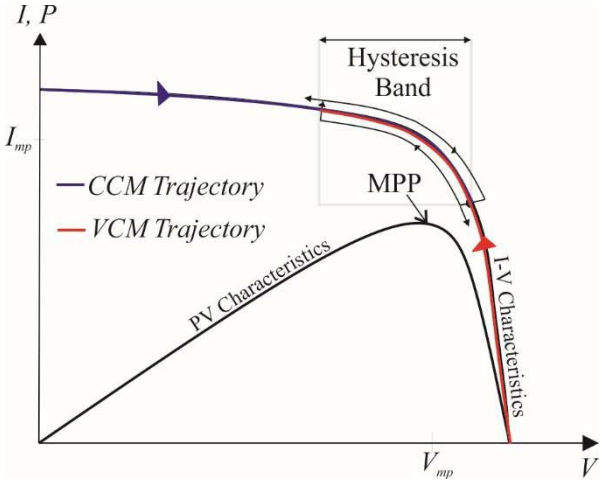

Fig. 4. Flowchart for simulator implementation algorithm using PV model.

front-end GUI is available for the user on the host computer, which takes the parameters like insolation, temperature, current, and voltage, and also has the provision of accepting the values in the form of input–output relations or lookup tables. Furthermore, the programmable electronic load is built with microcontroller ATMEGA 16, which can be programmed to obtain the smooth PV characteristics.

III. Control Scheme for Dual Mode Simulator

Fig. 4 shows the flowchart of the code executed by digital controller and mode selector operator. In this flowchart, the CCM and VCM are selected by monitoring the PV panel voltage and the voltage at maximum power point. The hysteresis effect is not shown in the flowchart. When measured PV voltage is less than the voltage at the maximum power point, the controller operates in CCM, and when measured

Authorized licensed use limited to: Instituto Tecnologico de Costa Rica (ITCR). Downloaded on June 23,2021 at 22:29:15 UTC from IEEE Xplore. Restrictions apply.

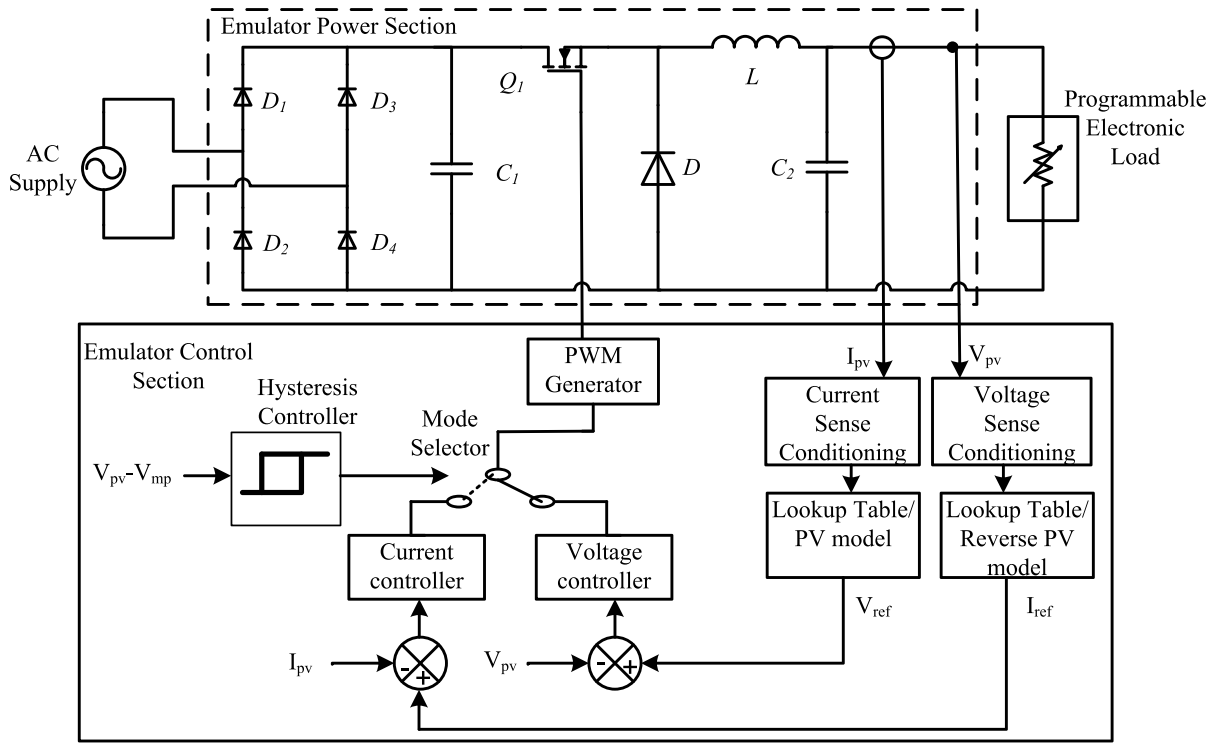

Fig. 5. Hysteresis nonlinearity in between CCM and VCM.

PV voltage is greater than the voltage at the maximum power point, the controller operates in VCM. The process of calculating the reference PV voltage and current is as follows.

Neglecting shunt resistance of PV cell, the equation for the reference PV current can be written as

$$I = I_{\text{ph}} - I_s \left[\exp\left(\frac{q(V + IR_s)}{AkT} \right) - 1 \right]. \tag{5}$$

A numerical method like the Newton–Raphson iterative method can be applied to the above-mentioned equation to calculate the PV current from the PV voltage when the simulator is in CCM.

The same equation can be rearranged for calculation of reference PV voltage from measured PV current when the simulator is in VCM

$$V = V_t \log_e \left[1 + \frac{I - I_{\text{ph}}}{I_s} \right] - IR_s. \tag{6}$$

During run time, the digital controller measures the simulator output voltage or output current and reference PV current or reference PV voltage, respectively, from the PV characteristic equations.

For calculation of current from (5), the measured output voltage of PV simulator need to be divided by total number of series connected cells N_s in the module to get individual cell voltage V. Similarly after calculation of voltage from (6), this calculated reference PV cell output voltage V need to be multiplied by total number of series connected cells N_s in the module to get total reference PV output voltage.

Neglecting the series resistance R_s, PV panel power P can be calculated as follows:

$$P = VI = VI_{\text{ph}} - VI_s \left[\exp\left(\frac{qV}{AkT} \right) - 1 \right]. \tag{7}$$

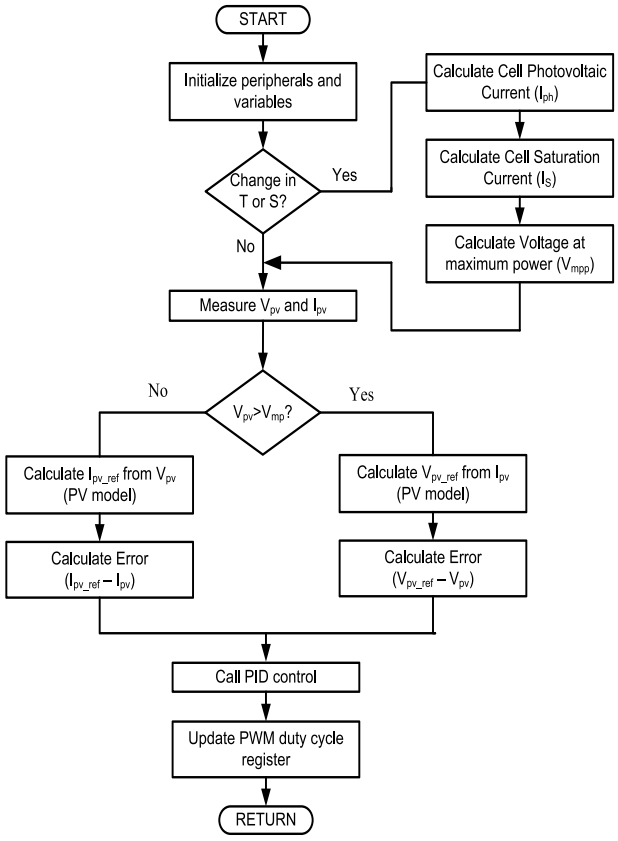

Fig. 6. Schematic of PV simulator design.

Authorized licensed use limited to: Instituto Tecnologico de Costa Rica (ITCR). Downloaded on June 23,2021 at 22:29:15 UTC from IEEE Xplore. Restrictions apply.

Fig. 7. Simulator complete test setup.

TABLE I
SIMULATOR PARAMETERS

Parameters	Values
Input DC voltage (V_{in})	100 V
Output DC voltage (V_0) range	0 - 70 V
Maximum Power (*3 series connected panel of 65W)	280 W
Switching frequency (f)	10 KHz
Inductor (L)	500 µH
Capacitor (C)	1000 µF

TABLE II
PV MODEL PARAMETERS

Parameters	Values
Reference Temperature (T_1)	25 ^0C
Number of Series cells (N_s)	36
Module open circuit voltage (V_{ocr})	21.06 V
Module short circuit current (I_{scr})	3.8 A
Short circuit current temperature coefficient (k_i)	0.0024
PN junction ideality factor (A)	1.2
Band gap voltage of the semiconductor (V_g)	1.12 eV

The voltage at maximum power point $V_{\rm mp}$ can be calculated by setting $dP/dV = 0$

$$\exp\left(\frac{qV_{\rm mp}}{AkT}\right)\left[\frac{qV_{\rm mp}}{AkT}+1\right]=\frac{I_{\rm ph}+I_s}{I_s}. \tag{8}$$

Solving above-mentioned equation by using the Newton–Raphson method, $V_{\rm mp}$ is calculated, which is used for determination of control mode. To get the fast dynamic response, the compensators for both modes are designed by using transfer function of the buck converter in respective mode.

The transition between the two modes, CCM and VCM, is decided based on terminal voltage $V_{\rm pv}$ and voltage at maximum power $V_{\rm mp}$. If control mode selection is decided by $V_{\rm pv} - V_{\rm mp}$ as positive or negative, i.e., on bang-bang control, then $V_{\rm pv}$ corresponds to $V_{\rm mp}$ in most of the MPPTs. In such cases, the control mode selection will always remain on the boundary of CCM and VCM. Therefore, hysteresis band is introduced in the region of $V_{\rm mp}$ so that chattering between the two modes can be avoided. Fig. 5 shows the effect of the introduction of hysteresis band in the selection of CCM and VCM. The primary reason for introducing hysteresis band is that the operating point of PV characteristics is MPP. Any slight variations in operating point shall change the region and the operating point may change the region rapidly and will result in chattering.

IV. DEVELOPMENT OF PV SIMULATOR HARDWARE

The circuit diagram and corresponding control strategy to control the output of the converter in order to obtain the PV characteristics are drawn schematically in Fig. 6. As explained in Section III, the accurate PV characteristics can be obtained in two regions using CCM and VCM without any fear of getting stuck in any one of the modes. Table I shows the parameters of the simulator circuit and Table II shows the parameters of PV module considered for hardware implementation. The real-time results are obtained by implementing the

Authorized licensed use limited to: Instituto Tecnologico de Costa Rica (ITCR). Downloaded on June 23,2021 at 22:29:15 UTC from IEEE Xplore. Restrictions apply.

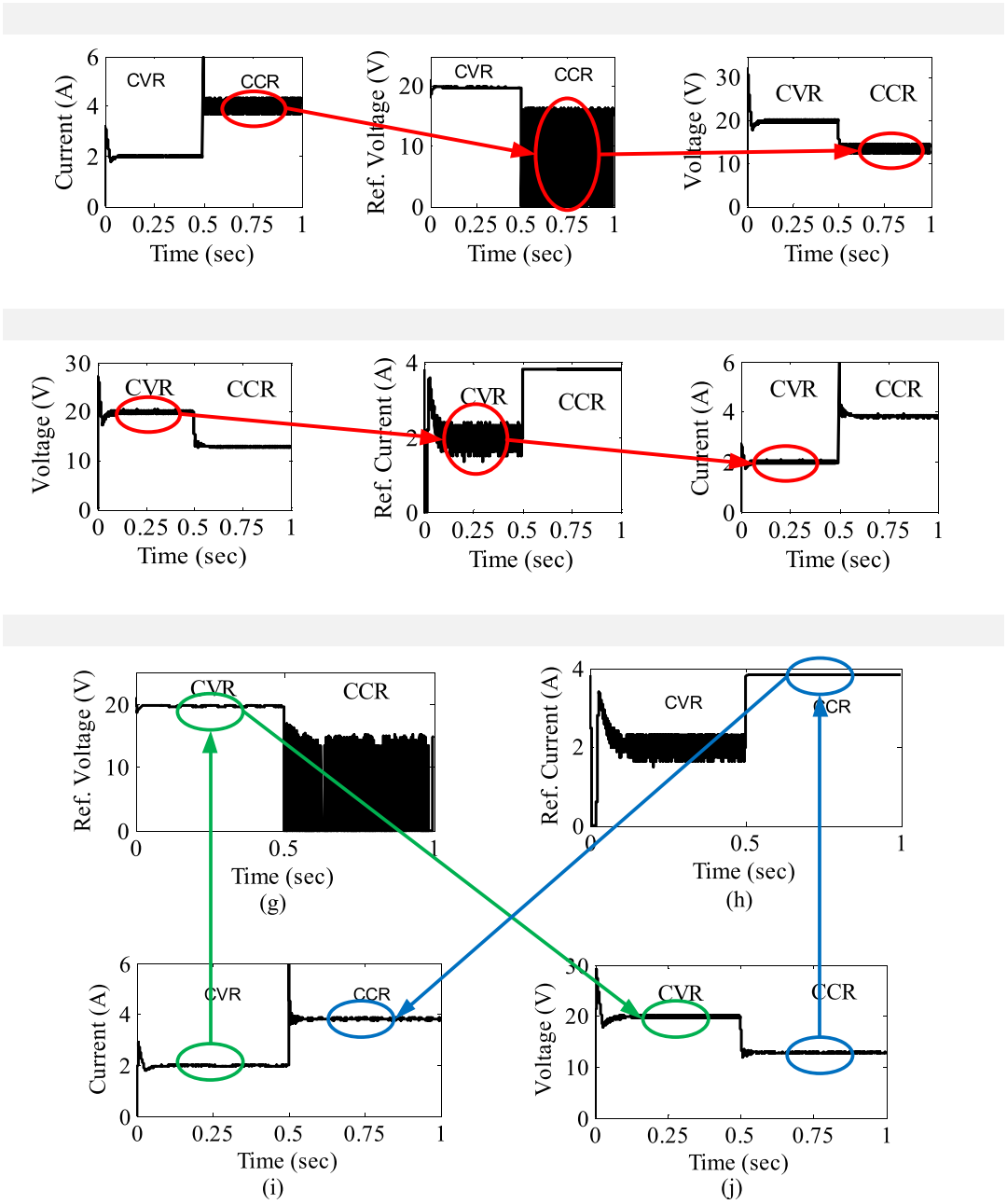

Fig. 8. Step change in load and transition between control modes (a)-(c) VCM waveforms (d)-(f) CCM waveforms (g)-(j) DCM waveforms.

controllers on the dsPIC33FJ32M202 digital signal controller for the proposed converter.

The dsPIC33EP32MC202 is a 28-pin, 16-b digital signal controller by microchip, which contains a reduced instruction set computer CPU, Modified Harvard architecture, C compiler optimized instruction set with 16-b wide data path, 24-b wide instructions, and 40-b accumulator. It has enhanced set of peripherals, which help in the implementation of real-time system like an emulator. Few of these enhanced peripherals include 10-b ADC, high-speed PWM, and 32-b timers/counters.

The digital signal controller is configured to operate at 60 MIPS operating frequency. The PWM switching frequency is set to 10 kHz, and the control loop is set at every 100 μs. Within this time period, controller is capable of sensing voltage and current signals, calculating reference voltage or current value from a mathematical model of PV cell and executing PID algorithm. Provision has also been made for the selection of lookup table-based or analytical-based mathematical model for implementation of I–V characteristics.

The complete test setup photograph of the emulator is shown in Fig. 7. Fig. 7 also shows the photograph of emulator control card, which has the provision of current and voltage sensing and digital signal controller section of the electronic load, which is used for dynamic loading of emulator circuit and is also shown separately in Fig. 7.

Authorized licensed use limited to: Instituto Tecnologico de Costa Rica (ITCR). Downloaded on June 23,2021 at 22:29:15 UTC from IEEE Xplore. Restrictions apply.

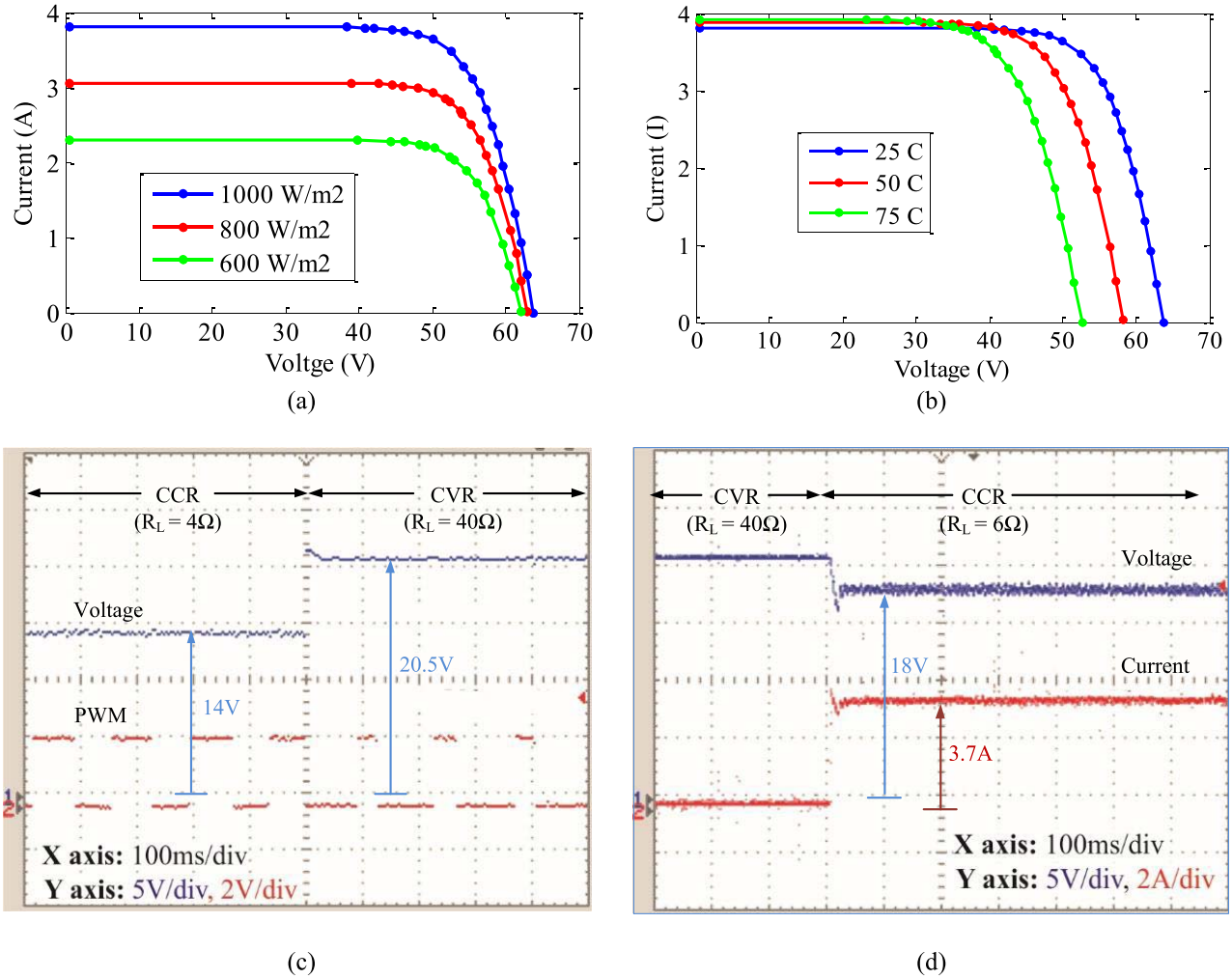

Fig. 9. Experimental results. (a) I–V characteristics for different insolations. (b) I–V characteristics at different temperatures. (c) Voltage and PWM wave for step change in load. (d) Voltage and current wave for transition between control modes.

V. Simulation and Experimental Results

The MATLAB-based simulation results for a step change in load and transition between control modes are shown in Fig. 8. Initially, a load of resistance 10 Ω is connected across simulator output. A step change in load from 10 to 3.33 Ω is applied at 0.5 s. When load resistance is 10 Ω, it is operating in the CVR of I–V characteristics. Whereas, when the load resistance is 3.33 Ω, it is operating in the CCR of IV characteristics.

A. Voltage Control Mode

In VCM, the output current of the simulator is fed as input to an analytical model of PV module, which calculates reference voltage corresponding to the input current. This reference voltage is compared with actual voltage, and this error difference is fed to the voltage controller. Fig. 8(a) shows simulator current signal from which the reference voltage signal is generated. Fig. 8(b) shows reference voltage signal, which has fewer distortions in the CVR, but it has considerable distortion in CCR. The simulator works well in VCM when it is operating in CVR. But when the simulator is operating in CCR, for a small change in current, there is a huge change in output reference voltage. So there is a considerable ripple on output voltage in CCR as shown in Fig. 8(c).

B. Current Control Mode

In CCM, the output voltage of simulator is fed as input to an analytical model of PV module, which calculates current reference corresponding to the input voltage. This reference current is compared with actual current, and this error difference is fed to the current controller. Fig. 8(d) shows simulator voltage signal from which the reference current signal is generated. Fig. 8(e) shows reference current signal, which has fewer distortions in CCR, but it has considerable distortion in CVR. The simulator works well in CCM when it is operating in CCR. But when the simulator is operating in CVR, for a small change in voltage, there is a huge change in output reference current. So there is a considerable ripple on output current in CVR as shown in Fig. 8(f).

C. Dual Control Mode

In dual control mode (DCM), hysteresis controller is used in between the CCM and VCM as a transition between two modes. If simulator output voltage is less than $V_{mp,}$ then it

Authorized licensed use limited to: Instituto Tecnologico de Costa Rica (ITCR). Downloaded on June 23,2021 at 22:29:15 UTC from IEEE Xplore. Restrictions apply.

operates in CCM, and if simulator output voltage is more than V_{mp}, then it operates in VCM. Fig. 8(g) and (h) shows reference current and reference voltage signals generated by the analytical model of PV module. The current reference signal has fewer distortions in CCR, whereas voltage reference signal has fewer distortions in CVR. So in CCR, CCM works well, and in CVR, VCM works well. Fig. 8(i) and (j) shows simulator current and voltage waveforms, which are superior to current and voltage waveforms of DCMs.

In order to experimentally test PV simulator at different load conditions, an electronic load is developed. The electronic load has multiple power transistors connected in parallel and biased in linear mode. This electronic load can be configured in current control or resistance control mode. With these two modes, it is possible to test PV Simulator at different current loads or different load resistance conditions.

For steady state analysis, PV Simulator is configured to work as three series-connected PV panels. Initially, testing is carried out by keeping the same temperature and insolation settings for all three PV panels. Then testing is carried out for different insolation settings for all three PV panels. Fig. 9(a) shows the captured steady-state I–V characteristics of PV Simulator for insolation of 1000, 800, and 600 W/m^2 for all three PV panels with a temperature of 25 °C; whereas Fig. 9(b) shows the captured steady-state I–V characteristics of PV Simulator for the temperature of 25 °C, 50 °C, and 75 °C for all three PV panels with insolation of 1000 W/m^2. The proposed solar simulator can also be configured for producing characteristics under partial shading conditions also.

For dynamic analysis, PV Simulator is configured to work as single PV panel of 65 W. Fig. 9(c) shows the variation in output voltage and PWM duty cycle of the simulator with respect to step change in load from 4 to 40 Ω. Fig. 9(d) shows experimental results of variation in output current and the output voltage of the simulator with respect to step change in load from 40 to 6 Ω. When load resistance is 40 Ω, the simulator is operating in CVR, and when the load resistance is 6 Ω, the simulator is operating in CCR. This step change in load shows the seamless transition of the controller from VCM and CCM.

VI. Conclusion

In this paper, a practical design approach for modeling and hardware implementation of a low-cost solar simulator has been investigated. The practical conditions like insolation and temperature are reproduced in PV characteristics variations. Selection of control mode for stable operation of the simulator in constant current and CVR of I–V characteristics of PV panel is implemented through a novel control approach, which works satisfactorily for the low-cost dsPIC processor. The control mode transition results into low ripple output voltage and current of the simulator. Hysteresis controller helps in a seamless transition of control modes near MPP. The proposed emulator can be useful for testing of various converters used for distributed generation and smart grid applications.

References

[1] B. H. Khan, *Non-Conventional Energy Resources*. New Delhi, India: Tata McGraw-Hill, 2006.

[2] S. J. Chiang, K. T. Chang, and C. Y. Yen, "Residential photovoltaic energy storage system," *IEEE Trans. Ind. Electron.*, vol. 45, no. 3, pp. 385–394, Jun. 1998.

[3] H. L. Tsai, C. S. Tu, and Y. J. Su, "Development of generalized photovoltaic model using MATLAB/SIMULINK," in *Proc. World Congr. Eng. Comput. Sci.*, 2008, pp. 1–6.

[4] M. G. Villalva, J. R. Gazoli, and E. R. Filho, "Comprehensive approach to modeling and simulation of photovoltaic arrays," *IEEE Trans. Power Electron.*, vol. 24, no. 5, pp. 1198–1208, May 2009.

[5] E. Koutroulis, K. Kalaitzakis, and N. C. Voulgaris, "Development of a microcontroller-based, photovoltaic maximum power point tracking control system," *IEEE Trans. Power Electron.*, vol. 16, no. 1, pp. 46–54, Jan. 2001.

[6] T. Esram and P. L. Chapman, "Comparison of photovoltaic array maximum power point tracking techniques," *IEEE Trans. Energy Convers.*, vol. 22, no. 2, pp. 439–449, Jun. 2007.

[7] W. Xiao and W. G. Dunford, "A modified adaptive hill climbing MPPT method for photovoltaic power systems," in *Proc. IEEE 35th Annu. Power Electron. Specialists Conf. (PESC)*, vol. 3. Jun. 2004, pp. 1957–1963.

[8] S. Mehrnami and S. Farhangi, "Innovative decision reference based algorithm for photovoltaic maximum power point tracking," *J. Power Electron.*, vol. 10, no. 5, pp. 528–537, 2010.

[9] H. Patel and V. Agarwal, "Maximum power point tracking scheme for PV systems operating under partially shaded conditions," *IEEE Trans. Ind. Electron.*, vol. 55, no. 4, pp. 1689–1698, Apr. 2008.

[10] M. Park and I.-K. Yu, "A novel real-time simulation technique of photovoltaic generation systems using RTDS," *IEEE Trans. Energy Convers.*, vol. 19, no. 1, pp. 164–169, Mar. 2004.

[11] A. Koran, K. Sano, R. Y. Kim, and J. S. Lai, "Design of a photovoltaic simulator with a novel reference signal generator and two-stage LC output filter," *IEEE Trans. Power Electron.*, vol. 25, no. 5, pp. 1331–1338, May 2010.

[12] A. Koran, T. LaBella, and J.-S. Lai, "High efficiency photovoltaic source simulator with fast response time for solar power conditioning systems evaluation," *IEEE Trans. Power Electron.*, vol. 29, no. 3, pp. 1285–1297, Mar. 2014.

[13] R. G. Wandhare and V. Agarwal, "A low cost, light weight and accurate photovoltaic emulator," in *Proc. 37th IEEE Photovolt. Specialists Conf. (PVSC)*, Jun. 2011, pp. 1887–1892.

[14] J. Chavarria, D. Biel, F. Guinjoan, A. Poveda, F. Masana, and E. Alarcón, "Low cost photovoltaic array emulator design for the test of PV grid-connected inverters," in *Proc. 11th Int. Multi-Conf. Syst., Signals Devices (SSD)*, Feb. 2014, pp. 1–6.

[15] C. H. Chang, E. C. Chang, and H. L. Cheng, "A high-efficiency solar array simulator implemented by an LLC resonant DC-DC converter," *IEEE Trans. Power Electron.*, vol. 28, no. 6, pp. 3039–3046, Jun. 2013.

[16] C. H. Chang, C. A. Cheng, and H. L. Cheng, "Modeling and design of the LLC resonant converter used as a solar-array simulator," *IEEE J. Emerg. Sel. Topics Power Electron.*, vol. 2, no. 4, pp. 833–841, Dec. 2014.

[17] M. C. Di Piazza, M. Pucci, A. Ragusa, and G. Vitale, "Analytical versus neural real-time simulation of a photovoltaic generator based on a DC–DC converter," *IEEE Trans. Ind. Appl.*, vol. 46, no. 6, pp. 2501–2510, Nov. 2010.

[18] M. T. Iqbal, M. Tariq, and M. S. U. Khan, "Fuzzy logic control of buck converter for photovoltaic emulator," in *Proc. 4th Int. Conf. Develop. Renew. Energy Technol. (ICDRET)*, 2016, pp. 1–6.

[19] A. V. Rana and H. H. Patel, "Current controlled buck converter based photovoltaic emulator," *J. Ind. Intell. Inf.*, vol. 1, no. 2, pp. 91–96, 2013.

[20] W. Zhang, and J. W. Kimball, "DC-DC converter based photovoltaic simulator with a double current mode controller," in *Proc. IEEE Power Energy Conf. Illinois (PECI)*, Feb. 2016, pp. 1–6.

[21] D. D. Lu and Q. N. Nguyen, "A photovoltaic panel emulator using a buck-boost DC/DC converter and a low cost micro-controller," *Solar Energy*, vol. 86, no. 5, pp. 1477–1484, 2012.

[22] M. Balato, L. Costanzo, D. Gallo, C. Landi, M. Luiso, and M. Vitelli, "Design and implementation of a dynamic FPAA based photovoltaic emulator," *Solar Energy*, vol. 123, pp. 102–115, Jan. 2016.

[23] M. Azharuddin, T. S. Babu, N. Bilakanti, and N. Rajasekar, "A nearly accurate solar photovoltaic emulator using a dSPACE controller for real-time control," *Electr. Power Compon. Syst.*, vol. 44, no. 7, pp. 774–782, 2016.

Authorized licensed use limited to: Instituto Tecnologico de Costa Rica (ITCR). Downloaded on June 23,2021 at 22:29:15 UTC from IEEE Xplore. Restrictions apply.

[24] T. D. Mai, S. De Breucker, K. Baert, and J. Driesen, "Reconfigurable emulator for photovoltaic modules under static partial shading conditions," *Solar Energy*, vol. 141, pp. 256–265, Jan. 2017.
[25] Y. Kim, W. Lee, M. Pedram, and N. Chang, "Dual-mode power regulator for photovoltaic module emulation," *Appl. Energy*, vol. 101, pp. 730–739, Jan. 2013.

Umesh K. Shinde (M'16) received the B.E. degree in electrical engineering from the Government College of Engineering at Karad, Shivaji University, Kolhapur, and the M.E. degree in control systems from the Government College of Engineering, Pune University, Pune, India. He is currently pursuing the Ph.D. degree with the Yeshwantrao Chavan College of Engineering, Nagpur, India.

He has 13 years of teaching experience and three years of industrial experience. He is currently an Assistant Professor with the Department of Electrical Engineering, Bhivarabai Sawant College of Engineering and Research, Pune. His current research interests include power electronic converters and renewable energy.

Sumant G. Kadwane (M'09–SM'16) received the B.E. degree in electrical engineering from the Yeshwantrao Chavan College of Engineering, Yeshwantrao Chavan College of Engineering, Nagpur University, Nagpur, India, the M.E. degree in control systems from the Government College of Engineering, Pune University, Pune, India, and the Ph.D. degree in engineering from the Birla Institute of Technology (BIT), Mesra, India.

He was a Faculty Member with the Department of Electrical and Electronics Engineering, BIT, Mesra, for seven years. He is currently a Professor with the Department of Electrical Engineering, Nagpur University, Nagpur, India, where he is teaching both UG and PG students. He has guided over 25 PG students with various control and DSP-based projects. His current research interests include control system design, power electronic converters, and renewable energy.

Dr. Kadwane is a member of IE(I) and ISTE. He is the Editor-in-Chief of the *Journal for Research in Engineering and Applied Sciences* Published from central India.

Ritesh Kumar Keshri (A'08–GS'10–M'10–SM'15) received the bachelor's and master's degrees from NIT, Jamshedpur, India, and the Ph.D. degree from the University of Padova, Padua, Italy.

He is currently with the Department of Electrical Engineering, Visvesvaraya National Institute of Technology, Nagpur, India, as an Assistant Professor. Dr. Keshri was with BIT Mesra, Ranchi as an Assistant Prfoessor from 2006 to 2015. His current research interests include power electronics and electric drives for electric vehicle propulsion and renewable.

Dr. Keshri received a silver medal for being first in M. Tech (electrical) in 2007, the Young Researcher Fellowship from the Ministry of University of Italy in 2008, the Erasmus Mundus Fellowship for Ph.D. from European Union in 2010, First Prize as a Student Team Leader of the University of Padova in class-3 of Formula Electric and Hybrid in 2011, and the 2016 Best Paper Award of the IEEE TRANSACTION ON INDUSTRIAL ELECTRONICS. He is associated with IEEE-IES, and IEEE-PELS, and contributed as organizing chairs for technical track and special sessions in IECON since 2013. He has been the Chair of Conference activities for the Technical Committee on Transportation Electrification of the Industrial Electronics Society (TCTE) IEEE from 2014 to 2015 and is associated as a Secretary of TCTE-IES and Chair Sub-Committee for EV/HEV/FCEV of TCTE.

S. P. Gawande (M'16) received the B.E. degree in electrical engineering and the M.Tech degree in integrated power system from Nagpur University, Nagpur, India, and the Ph.D. degree from Visvesvaraya National Institute of Technology, Nagpur.

He has 13 years of teaching experience and is working currently as Assistant Professor in the Department of Electrical Engineering, Yeshwantrao Chavan College of Engineering, Nagpur. He has authored over 50 papers in reputed peer reviewed journals like IEEE Transactions, IET, and Elsevier and IEEE conferences, such as PEDES, IECON, PESC, and INDICON. His current research interest includes power electronics, FACTS, power quality, and power electronics applications to renewable energy systems.

Dr. Gawande is a Life Member of ISTE and IACSIT, and a member of Institution of Engineers, India. He is an Editor of the *Journal of Electrical and Power System Engineering*, the *Journal of Advances in Electrical Drives*, and the *Journal of Controller and Converter*. He is a Regular Reviewer of IEEE Transactions, IET, Elsevier, and Taylor and Francis, and for various reputed IEEE conferences, such as PEDES, IECON, CIGRE, and PES Winter meetings.

Authorized licensed use limited to: Instituto Tecnologico de Costa Rica (ITCR). Downloaded on June 23,2021 at 22:29:15 UTC from IEEE Xplore. Restrictions apply.